Barking up the Wrong Tree? Multifamily Housing and Tree Loss: Evidence from Los Angeles

Michael Pham

May 2025

Working Paper

This paper evaluates how the construction of multi-family properties in Los Angeles affect the neighborhood characteristic nearby as defined as greenery coverage. I create address-level panel data by employing computer vision techniques applied to street-level imagery and use difference-in-differences estimators. I find that multi-family development has no negative effect on nearby tree and greenery coverage and may even contribute to a modest increase, with estimates indicating a statistically significant 2.3% rise in total greenery (trees and shrubs) coverage.

1 Introduction

The percentage of cost-burdened renter households, households that spend over 30% of income on housing, was 46.8% in 2017 (Dumont, 2019). Hot housing markets such as those of Los Angeles are even more unaffordable. As of April 2025, the average rent in Los Angeles is $2,333 per month, which is about 28% higher than the national average (Zillow, 2025). Despite this, in the first half of 2024, Los Angeles only issued permits for 5,208 residential units (Urbanize LA, 2024).

Los Angeles and other major U.S. cities face a housing shortage, yet new housing developments are frequently opposed by local residents. Economists have found that local housing resistance, often called NIMBY ("Not in my backyard"), can substantially slow down, make projects more expensive, or completely shut down new housing construction (Karandikar, 2024). Residents commonly cite concerns over traffic, parking, and, increasingly, more subjective notions such as "neighborhood character." Tiebout sorting theory suggests that residents "vote with their feet" by moving to communities that best match their preferences for public goods and local regulations. Zoning laws, particularly ones such as minimum lot sizes or single-family zoning, are often implemented to limit construction of multi-family housing, a way of barring lower-income individuals into the community (Tiebout, 1956). This does seem to work as more zoning laws make housing more expensive, which keeps housing communities homogeneous (Glaeser and Gyourko, 2003).

Los Angeles has recently tried to relax these zoning laws. Measure JJJ was passed Los Angeles in 2016. Measure JJJ incentivized multifamily project by offering streamlined permits for multifamily with low-income units in Transit Oriented Communities (TOC), areas near public transport. However, the majority of Los Angeles still falls outside of the TOC zones affected by Measure JJJ. Zoning laws give disproportionate power to incumbent residents. While residents in Los Angeles don't have direct veto power, they can vote in local City Council officials who control zoning. They can also voice their opposition at public discretionary approval process hearings. During Los Angeles City Planning Commission housing hearings, one of the most frequently voiced objections to proposed projects is the preservation of "neighborhood character". Using text data from these hearings, I apply sentence embedding using a sentence embedding transformer (Wang et al., 2020), followed by K-means clustering, to classify "neighborhood character" comments (details in Appendix). I find that approximately 23% of comments concerning neighborhood character focus specifically on "preserving the existing neighborhood amidst new developments" (Kestelman, 2025). This rhetoric is notably vague. Further subsetting these "preserving the existing neighborhood amidst new developments" comments, I observe that a significant fraction of residents specif-

ically express concerns about the loss of trees greenspace, and open space resulting from new construction projects.

The production of multifamily housing does produce both positive and negative externalities not internalized by the developers of multifamily housing. New developments can generate externalities by affecting nearby home values, traffic congestion, parking infrastructure, crime rates, and economic revitalization. The effects of constructing multifamily and affordable housing have been previously studied, though much of the literature has focused on outcomes on nearby rent prices, neighborhood composition, and crime. For example, (Asquith et al., 2020) examine the impact of new market-rate housing on neighborhood composition and rental prices using a difference-in-differences model. They define the treatment zone as within 250 meters of new developments and use the 250–600 meter radius as a control group. Their findings suggest that in low-income neighborhoods, market-rate construction decreases rents by 5–7% and increases out-migration from lower-income households. Similarly, (Li, 2022) studies New York City and find that a 10% increase in housing stock leads to a 1% reduction in local rents, increases the number of nearby restaurants, and does not lead to displacement of existing residents.

Although these studies focus on market-rate housing, a parallel literature has examined the Low-Income Housing Tax Credit (LIHTC) program, the largest federal initiative supporting the development of affordable rental housing. Under LIHTC, the federal government allocates tax credits to states, which then distribute them to developers who commit to setting aside units for low-income tenants. As a result, LIHTC developments are typically multifamily in form. (Diamond and McQuade, 2017) employ a non-parametric spatial difference-in-differences model to assess the effects of LIHTC developments. They find that in low-income neighborhoods, LIHTC construction increases nearby property values and reduces crime. However, in high-income areas, LIHTC developments reduce property values by approximately 2.5% and attract migration from lower-income residents. Similarly, (Baum-Snow and Marion, 2009) find LIHTC developments in neighborhoods at the 30th percentile of income are associated with a 5% decline in local housing prices.

Outcomes may have been previously limited to housing prices, composition, and crime likely due to the limited availability of fine-grained, spatial data. However, advances in big data and machine learning techniques have opened new avenues for studying more nuanced forms of neighborhood change, such as gentrification. Recently, Yelp review data has been used to track gentrification through changes in commercial activity (Glaeser et al., 2018). More recently, the rise of computer vision (CV) and deep learning methods has enabled researchers to quantify visual and otherwise unmeasurable neighborhood attributes at scale. (Huang et al., 2022) train a CV algorithm that detects signs of gentrification from changes in

Google Street View images. Similarly, (Naik et al., 2014) introduce Streetscore, a user-rated computer vision model that quantifies perceived safety from street-level imagery, providing another lens through which to assess neighborhood change. There have been no studies to date on the causal effects of multifamily housing on tree coverage itself. As such, it remains unclear whether local residents' concerns about loss of tree coverage reflect genuine environmental considerations or whether they function as unverifiable objections used to oppose new housing developments. In this paper, I use new CV methods and event study estimators to investigate whether these concerns are substantiated. Specifically, I ask: *Does building multifamily housing result in a measurable loss of greenery and tree coverage?*

2 Data

2.1 Urbanize LA

I first web scrape the Urbanize LA (https://la.urbanize.city/) website in order to acquire information on where multifamily projects are being built in Los Angeles and project level data. Urbanize LA is a housing site that documents residential and non-residential projects in Los Angeles and other major U.S. cities. For each proposed project, the site information on location, development type, other proposed project statistics, and also various articles about the project. I use the address provided in each article to geocode projects to latitude and longitude coordinates, and extract additional project characteristics to use as covariates in my analysis such as number of floors above ground, total ousing units, and building construction type. Urbanize LA does not include information on the exact date the project was proposed nor constructed. However, Urbanize LA frequently publishes articles on the projects, with the first being around the time they are proposed. I use the publication date of the earliest article as a proxy for timing treatment. While this approach likely introduces some measurement error, it offers a consistent method for dating new developments. I scraped the data in February 2025 (Kestelman, 2025). Urbanize LA contains information on 3,803 development projects, but I restrict the sample to those coded as condominiums, townhouses, or apartments, with at least two units, proposed between 2014 and 2021, and marked as either approved or under construction or completed, excluding projects with multiple overlapping proposals. After applying these filters, the final sample includes 1022 unique multi-family developments.

2.2 Google Streetview

I use Google Map's Static Street View API to acquire street-level imagery at various locations across time, called "panoramas" (See appendix for methodology). I identify 2,120,682 potential panorama-time location pairs from Google Street View within a 1200m grid of the housing developments of interest - of which approximately 145,246 panoramas at 27,530 different locations are used in the final analysis.

2.3 Greenery Coverage

In order to assess tree and greenery coverage, I use the Segformer-B5 model, a computer vision architecture that performs semantic segmentation, on the Google Static Street View images. Sementatic segmentation is a computer vision task that involves taking an input image and classifying each pixel into a pre-defined category. A common use case of semantic segmentation is how self-driving cars are able to "see" and categorize elements in its environment such as cars, roads, pedestrians, and other objects by assigning a class label to every pixel in the camera's view. The Segformer has a transformer-based encoder transforms the input image into a latent representation, or a set of hierarchical feature maps, and a Multi-Layer Perceptron decoder block that fuses these features to produce dense pixel-wise segmentation maps. The B5 variant is the largest Segformer model with approximately 84.8 million parameters. (Xie et al., 2021) (Vaswani et al., 2017)

I use a version of the Segformer-B5 with weights that have already been pre-trained on the Cityscapes Dataset, a dataset of pixel-level annotations for street-level video recorded in 50 different cities (Cordts et al., 2016). These pre-trained weights allow me to deploy the model in zero-shot without requiring additional training (NVIDIA, 2021). This model allows me to generate outcome variables based on the percentage of each Static Street View image containing by various greenery elements. Specifically, it can detect overall tree coverage as well as separately low-level vegetation and terrain. I manually label a few Static Street View images and record Segformer-B5 accuracy below.

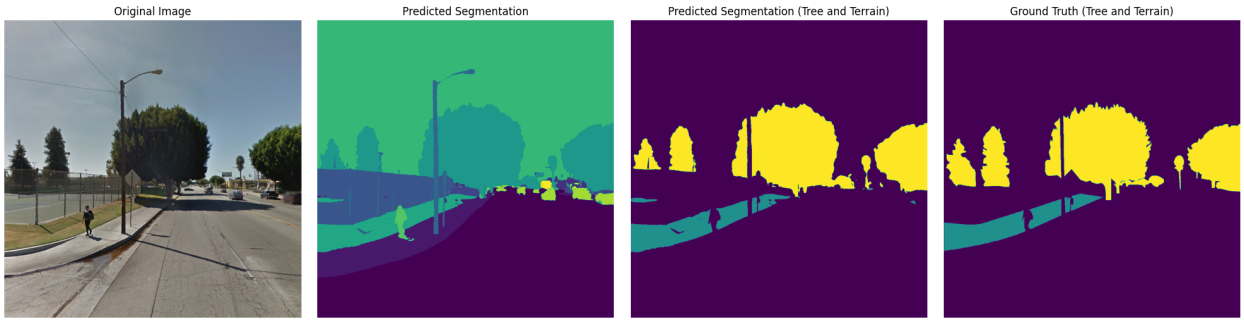

Figure 1: Original Image, Predicted Segmentation, Predicted Segmentation (Only Trees and Terrain), Ground Truth (Only Trees and Terrain). (Left to Right)

Table 1: Segmentation Performance Metrics (SegFormer-B5)

Class	**Accuracy**	**IoU**
Background	0.9760	0.9709
Terrain	0.9954	0.7894
Trees	0.9805	0.8902
Overall Accuracy	0.9840	
Mean IoU	0.8835	
Weighted Mean IoU	0.9538	

Accuracy is simply pixelwise-accuracy and Intersection over Union (IoU) measures overlap between the predicted area and the true area:

$$\text{IoU} = \frac{\text{TP}}{\text{TP} + \text{FP} + \text{FN}} \tag{1}$$

$$\text{Mean IoU} = \frac{1}{C} \sum_{i=1}^{C} \text{IoU}_i \tag{2}$$

where C is the set of all classes, $C = \{\text{tree}, \text{terrain}, \text{neither}\}$. [Authors] report a Single Scale Mean IoU of 0.824 on all Cityscape classes. These metrics on a few labeled Los Angeles streetview panoramas are in line with the Segformer-B5 accuracy metrics on the official Cityscape dataset despite no training.

There is inevitably some measurement error when estimating urban greenery coverage. However, with pixel-wise accuracy of 99.54% and 98.04% on terrain and trees, respectively, measurement error is unlikely to be a major concern.

3 Methodology

3.1 Ring Method General Model

Using the aforementioned data sources, I build a panel dataset. Each multifamily unit-panorama pair i is a unit of observation. Using the "ring method", unit-panorama pairs where the panorama is within 250 meters falls into the treatment group once the project is built ($Y_{it}^{d=1}$). Unit-panorama pairs where the panorama is 251-600 meters fall into the control group ($Y_{it}^{d=0}$). The baseline specification is

$$Y_{it} \;=\; \alpha_i \;+\; \lambda_t \;+\; \beta\, D_{it} \;+\; \varepsilon_{it}, \tag{3}$$

where α_i are unit fixed effects, λ_t are calendar-year fixed effects, and β is the average spatial-exposure effect of interest.

3.2 Spatial Ring Difference-in-Differences

Using panel data on projects that were proposed and "treated" or built between 2014 and 2021, I begin by applying staggered adoption difference-in-differences (DiD) estimators. Because I only observe a proxy for the start of a project, which likely occurs after public announcement but before construction begins, I hypothesize that if there is a sizeable treatment effect, it may not manifest in the first few years following "treatment." Instead, more clearly defined effects are likely to emerge later, once construction is completed or the project becomes operational, with potentially even greater heterogeneity over time. Given the possibility of heterogeneous treatment effects across periods, I employ more flexible DiD estimators that avoid mixing early-treated units into the control group for later-treated units, thereby mitigating issues related to "negative weighting." Specifically, I use the (Callaway and Sant'Anna, 2021) estimator and the Matrix Completion with Nuclear Norm Regularization (MCNNR) method developed by (Athey et al., 2017) to estimate treatment effects.

Using the Callaway and Sant'Anna (CS) estimator, I estimate the average treatment effect for the group treated in year g at time t as:

$$ATT(g,t) = E\left[\left(\frac{G_g}{E[G_g]} - \frac{\hat{p}(X)C}{E\left[\frac{\hat{p}(X)C}{1-\hat{p}(X)}\right]}\right)(Y_t - Y_{g-1})\right] \tag{4}$$

where

- $G_g = \mathbf{1}\{\text{unit first becomes exposed in year } g\}$;

- $C = \mathbf{1}\{\text{unit is not yet exposed at } t\}$;
- $\hat{p}(X)$ is the propensity score estimated from pre-treatment covariates X;
- $Y_{it} - Y_{i,g-1}$ denotes the outcome change relative to the last pre-treatment period.

This estimator ensures that each group is compared only to not-yet-exposed controls and adjusts for baseline covariate imbalance via propensity score weighting.

To complement the CS estimator, I also employ Matrix Completion with Nuclear Norm Regularization (MCNNR), which estimates missing counterfactual outcomes by treating the spatial-difference panel as a low-rank matrix-completion problem. Now a unit of observation is a housing unit. For each housing unit i, at time $t = \theta$ a multifamily house is built: units in the inner ring switch from the untreated potential outcome $Y_{it}^{d=0}$ for all $t < \theta$ to the treated potential outcome $Y_{it}^{d=1}$ for all $t \geq \theta$. Let $Y_{it}(1) = Y_{it}^{d=1,inner} - Y_{it}^{d=1,outer}$. Let $Y_{it}(0) = Y_{it}^{d=0,inner} - Y_{it}^{d=0,outer}$, The average treatment effect (ATE) is $E\big[Y_{it}(1) - Y_{it}(0)\big]$, but $Y_{it}(0)$ is unobserved for $t \geq \theta_i$. Following Athey et al., 2020, we impute these missing potential outcomes $Y_{it}(0)$ with matrix completion.

The actual matrix with all counterfactual urban green space coverages over time $Y(0)$ without covariates is computed by

$$Y_{N\times T} = L_{N\times T} + \epsilon_{N\times T} \tag{4}$$

an $N \times T$ matrix where N is the number of multifamily units as observations across the T periods of panel data. The matrix completion employs regularization, a penalty term added to the loss function. The regularization used by this method is the nuclear norm which encourages low-rank, where rank is linearly independent rows, solutions. This allows for the essential underlying patterns to be captured while minimizing overfitting.

$$\|L\|_* = \sum_{j=1}^{\min(N,T)} \sigma_j(L) \quad \text{where } \sigma_j(L) \text{ is the rank of } L \tag{5}$$

$$\min(L)\frac{1}{|O|}\sum_{(i,t)\in O}(Y_{it} - L_{it})^2 + \lambda_L\|L\|_* \tag{6}$$

With these "fat" matrixes where there is sufficient data over time, the vertical weighted averages of the control group units are used to model the missing counterfactuals for every unsolved period - this is essentially turning each observation into a synthetic control. The treatment effect is a weighted difference between the observed $Y(1)$ observed outcomes and

the computed counterfactual $Y(0)$:

$$\tau = \frac{\sum_{i,t} W_{it} \left(Y_{it}(1) - Y_{it}(0) \right)}{\sum_{i,t} W_{it}} \tag{7}$$

I test parallel trends with a pre-trends test. I fail to reject the null that the trends are parallel in the pre-treatment period.

Table 2: Pretreatment Trend Test (Null: All Pre-treatment Effects = 0)

Test Statistic	Value
$\chi^2(28)$	18.4240
p-value	0.9150

3.3 Exposure Method General Model

3.4 Non-Parametric Spatial Difference-in-Differences

A major limitation of the ring-based estimation method is that it does not account for spillover effects from nearby projects. Although I control for the presence of other proposed projects in the area, this approach cannot fully capture the influence that neighboring developments may have on local outcomes. To address this, I employ (not in this paper I don't, but I will in the future) a difference-in-differences estimator that is nonparametric and better suited to accommodate spatial spillovers.

Using the sample of 2,678 multi-family projects (defined as condominiums, townhouses, and apartments with two or more units), I find that the median project is located within 1200 meters of 21 other projects. This high density of developments implies substantial potential for spillover effects, making it essential to use methods that can flexibly model these interactions.

Table 3: Multi-family Projects within 1200m

Percentile	**Value**
25%	6
50% (Median)	21
75%	46

There is a growing literature in the spatial DiD space to touch up on this concern. Many require that (Diamond and McQuade, 2017) that the outcome, greenspace coverage, be a continous function wrt to distance away from the observations. (Xu, 2023) innovates

a method that doesn't build in this continuity assumption. Each unit of observation is a panorama spot i. Each unit is given an exposure level (g), which we first calculate as a simple count of all the multifamily unit houses within 600m at a given time t; also the weighted distance aggregate of all the units within 600m at time t. The expected direct ATE on the Treated at a given neighborhood exposure level (g) is

$$\tau(g) = \frac{1}{|D_M|} \sum_{i \in D_M} E\left[y_{i2}(1, w_{-i}) - y_{i2}(0, w_{-i}) \mid W_i = 1, G_i = g, z_i\right] \tag{8}$$

The spillover effect between exposure levels g and g' is given by

$$\frac{1}{|D_M|} \sum_{i \in D_M} \left(E\left[y_{i2}(1, w_{-i}) \mid W_i = 1, G_i = g, z_i\right] - E\left[y_{i2}(1, w'_{-i}) \mid W_i = 1, G_i = g', z_i\right]\right) \tag{9}$$

The doubly robust estimator for the direct effect at exposure level g is given by

$$\begin{aligned}\tau(g) = E_D \Bigg[& \frac{W_i}{\eta(z_i)} \left(\frac{1\{G_i = g\}}{\eta_{1g}(z_i)} (Y_{i2} - m_{i2,1g}(z_i)) - (Y_{i1} - m_{i1,1}(z_i)) \right) \\ & - \frac{1 - W_i}{1 - \eta(z_i)} \left(\frac{1\{G_i = g\}}{\eta_{0g}(z_i)} (Y_{i2} - m_{i2,0g}(z_i)) - (Y_{i1} - m_{i1,0}(z_i)) \right) \\ & + \Delta m_{i2,g}(z_i) - \Delta m_{i1}(z_i) \Bigg]\end{aligned} \tag{10}$$

4 Results

The Callaway and Sant'Anna (CS) method estimates an increase in tree coverage of 0.29 percentage points. To contextualize this effect, the average panorama location exhibited 10.95% tree coverage in the year prior to treatment. Thus, the estimated coefficient corresponds to approximately a 2.4% relative increase in tree coverage following nearby multifamily construction. However, this effect is not statistically significant and should be interpreted as a null result.

Two-way fixed effects model similary shows a null result. The Matrix Completion results are also presented, showing a positive coefficient, but null result. Although the matrix completion method acts as a robustness check, its results should be taken with a grain of salt. Due to data availability, the matrix compeltion method only takes into account treatment up until 2 periods after treatment (see Appendix).

Table 4: Average Tree Coverage Treatment Effect on Treated Areas (ATT)

	Callaway Sant'Anna	**Matrix Completion**	**TWFE**
Coefficient	0.2921	0.0833	-0.0466
Std. Err.	0.2168	0.1612	0.0575
P> $\|z\|$	0.178	0.605	0.418
95% CI	[-0.1329, 0.7170]	[-0.2262, 0.3889]	[-0.1594, 0.0661]

When results are disaggregated by dynamic periods, there is clear evidence of null effects in the pre-treatment years. Because the exact construction dates of multifamily projects are unknown, I rely on article publication dates as proxies. As permitting and construction typically take one to two years, it is expected that no measurable treatment effects would appear immediately following these proxy dates. By year 4, most projects are likely completed, and any environmental changes would be observable.

Standard errors remain relatively flat in the early pre-treatment years—likely due to limitations in data availability for earlier periods—and stay stable through the first two years following treatment. However, they increase substantially in years 3 to 4 post-treatment, coinciding with the likely construction window. This increase in uncertainty may reflect underlying heterogeneity in treatment effects: although the overall average effect of multifamily construction on greenery is null or slightly positive, some projects may lead to increased tree coverage while others may result in loss, depending on local conditions and project characteristics.

Table 5: CS Dynamic Tree Coverage Effects by Period

Per. to Treat	Coefficient	Std. Err.	z	P> $\|z\|$	95% CI Lower	95% CI Upper
-7	0.5724	0.6791	0.84	0.399	-0.7586	1.9034
-6	0.5264	0.4829	1.09	0.276	-0.4201	1.4729
-5	0.5364	0.4231	1.27	0.205	-0.2930	1.3657
-4	0.1924	0.3668	0.52	0.600	-0.5266	0.9114
-3	0.3848	0.3178	1.21	0.226	-0.2380	1.0077
-2	0.1921	0.2633	0.73	0.466	-0.3239	0.7083
-1	0.3433	0.2601	1.32	0.187	-0.1666	0.8532
0	0.3344	0.2581	1.30	0.195	-0.1772	0.8403
1	-0.0917	0.2327	-0.39	0.693	-0.5477	0.3643
2	0.3983	0.3731	1.07	0.286	-0.3329	1.1295
3	0.6501	0.3388	1.92	0.055	-0.0193	1.3141
4	0.4420	0.4152	1.06	0.287	-0.3718	1.2557
5	-0.6202	0.5376	-1.15	0.249	-1.6739	0.4334
6	1.0264	0.6130	1.67	0.094	-0.1750	2.2279
7	1.2411	0.6673	1.95	0.051	-0.0037	2.4866
8	-1.3162	0.7844	-1.68	0.093	-2.8569	0.2215
9	0.2275	1.0229	0.22	0.824	-1.7761	2.2311
10	-0.0292	1.3661	-0.02	0.983	-2.7066	2.6487

I then look at treatment effects of building multifamily housing on total greenery, which includes not only trees, but also low level vegetation, shrubs, and other non-tree greenery. The CS estimator finds a statistically significant increase of 0.4825 in total greenery coverage from multifamily housing. In the year before treatment, panorama spots had on average 12.39% total greenery coverage. A coefficient of 0.4825 would translate to a 2.3% increase in tree coverage from building multifamily housing.

Both Matrix Completion and Two-way fixed effects in constrast to the CS estimator show a negative coefficient, but a null result. However, a caveat with Matrix Completion is if there were treatment effects, we would expect that these show up after at least years 3-4 after construction. Due to data limitations, the Matrix Completion approach includes only two post-treatment periods, which may be insufficient to capture these delayed effects.

Table 6: Average Total Greenery Treatment Effect on Treated Areas (ATT)

	Callaway Sant'Anna	**Matrix Completion**	**TWFE**
Coefficient	0.4825**	-0.1869	-0.0255
Std. Err.	0.2412	0.1986	0.0616
P> $\|z\|$	0.045	0.347	0.679
95% CI	[0.0097, 0.9553]	[-0.5662, 0.1732]	[-0.1462, 0.0952]

Once again with treatment effects disaggregated by period, we see that standard errors widen after two periods after treatment and once again 5 periods after treatment.

Table 7: CS Dynamic Total Greenery Coverage Effects by Period

Per. to Treat	Coefficient	Std. Err.	z	P> $\|z\|$	95% CI Lower	95% CI Upper
-7	0.2064	0.7389	0.28	0.780	-1.2418	1.6546
-6	0.3959	0.5119	0.77	0.439	-0.6073	1.3992
-5	0.3525	0.4499	0.78	0.433	-0.5293	1.2343
-4	0.0391	0.3869	0.10	0.920	-0.7193	0.7974
-3	0.2408	0.3372	0.71	0.475	-0.4201	0.9016
-2	0.0780	0.2854	0.27	0.785	-0.4814	0.6375
-1	0.3841	0.3073	1.25	0.211	-0.2182	0.9865
0	0.3604	0.2883	1.25	0.211	-0.2047	0.9256
1	0.0728	0.2629	0.28	0.782	-0.4424	0.5880
2	0.8586	0.5264	1.63	0.103	-0.1731	1.8903
3	1.0178	0.3573	2.85	0.004	0.3174	1.7182
4	0.5264	0.4467	1.18	0.239	-0.3491	1.4020
5	-1.0777	0.5497	-1.96	0.050	-2.1551	-0.0002
6	1.6688	0.7221	2.31	0.021	0.2534	3.0841
7	1.5942	0.7053	2.26	0.024	0.2118	2.9765
8	-0.9658	0.8590	-1.12	0.261	-2.6494	0.7178
9	-0.1956	1.2429	-0.16	0.875	-2.6316	2.2404
10	0.5104	1.6704	0.31	0.760	-2.7636	3.7844

5 Conclusion

This analysis is subject to several endogeneity concerns and other concerns, some of which I begin to address below. As this is an early-stage paper, I also outline ways I will address these issues in future work.

There is possibly a self-selection issue where developers aren't building multifamily projects in random, exogenous locations. They could be building based on zoning incentives and profit incentives. Within profit incentives, developers tend to build in areas that are rapidly changing already and undergoing gentrification (cite). One potential solution is to use zoning reforms, such as the Measure JJJ Transit-Oriented Communities (TOC) policy or other exogenous zoning changes as instrumental variables, to isolate plausibly exogenous variation in multifamily construction.

There is potential measurement error arising from the use of computer vision algorithms to detect tree coverage. There are many factors which muddy the accuracy of actual tree/greenery coverage. One notable issue is obstruction by cars, which can partially block

the streetview image's view of surrounding greenery. Importantly, car presence may itself be endogenous to multifamily development (a potential avenue is that more developed areas tend to have higher vehicle density). I need to figure out a way to normalize tree coverage by cars.

Accuracy of the semantic segmentation algorithm aside, capturing the 3-dimensional nature of the real world with 2-dimensional street-view images is a source of measurement error. While there are advanced techniques to reconstruct more complete and three-dimensional representations of streets (cite), this analysis is constrained by data availability. Specifically, I am limited to locations with historical Google Street View panorama data, which provides only two-dimensional snapshots from fixed points in time and space. As a result, these images may not fully capture the three-dimensional structure and density of tree coverage in a given area.

Timing also presents some endogeneity concerns. There are also endogeneity concerns related to the timing and routing of Google Street View data collection. If Street View vehicles are more likely to capture images in certain neighborhoods at specific times of the year, this could bias measurements, particularly in areas with deciduous trees, which lose their leaves seasonally. Furthurmore, some areas at certain times could be affected by weather and nature, particularly forest fires.

A key limitation of using the 250m and 600m rings as treatment and control zones lies in the spatial resolution of the available data. Panorama points were sampled at a very wide every approximately 200 meters due to financial constrains on API calls I could make, which means that within the treatment zone, observations include both locations directly adjacent to the new building and others as far as 200 meters away—roughly the edge of the inner ring. For each building, I collect one panorama at the site and four additional panoramas located 200 meters away in each cardinal direction. As a result, much of the "treatment" data is located at the outer boundary of the treatment zone, potentially placing a lower bound on the estimated treatment effects. In future work, I will sample at smaller subgrids.

Arguably, the most pressing concern is spillover effects. As shown, a lot of mukltlifamily builds are locating close to each other. A simple ring spatial difference-in-differences method doesn't isolate the treatment effect of building. In order to have, I must implement such as Xu, 2025.

While some residents cite changes in greenery as indicative of shifts in neighborhood character, others refer more broadly to construction activity, gentrification, or redevelopment when expressing such concerns. In future work, I hope to extend this analysis to capture those additional dimensions of neighborhood change using construction, safety, and gentrification scores using computer vision methods such as those developed by (Huang et al., 2022) and

(Naik et al., 2014). Even if this paper finds no adverse effects on nearby tree or greenery coverage, it is possible that references to greenery serve as a proxy for other concerns. In some cases, appeals to changing "neighborhood character" may function as a coded way to express discomfort with changes in underlying ethnic, racial, or socioeconomic changes in the neighborhood .

It's important to note that there may be limited external validity. Los Angeles has a unique zoning, geography, and land use preferences. Findings from this analysis may not generalize to cities with different regulatory environments or urban development patterns. While this is an early-stage analysis with several components still in development, the paper contributes to the literature by introducing a scalable method for applying computer vision algorithms to extract and analyze spatial information from street-level imagery. The other contribution is that I find is that in a model that treats multifamily construction as exogenous and does not account for potential spillover effects, preliminary results suggest that building multifamily housing in Los Angeles leads to a 2.4% increase in tree coverage and a statistically significant 2.3% increase in total greenery.

References

Asquith, B. J., Mast, E., and Reed, D. (2020). Supply shock versus demand shock: The local effects of new housing in low-income areas. *SSRN Electronic Journal*.

Athey, S., Bayati, M., Doudchenko, N., Imbens, G., and Khosravi, K. (2017). Matrix completion methods for causal panel data models. *arXiv preprint arXiv:1710.10251*.

Baum-Snow, N. and Marion, J. (2009). The effects of low income housing tax credit developments on neighborhoods. *Journal of Public Economics*, 93(5-6):654–666.

Callaway, B. and Sant'Anna, P. H. C. (2021). Difference-in-differences with multiple time periods. *Journal of Econometrics*, 225(2):200–230.

Cordts, M., Omran, M., Ramos, S., Rehfeld, T., Enzweiler, M., Benenson, R., Franke, U., Roth, S., and Schiele, B. (2016). The cityscapes dataset for semantic urban scene understanding. In *Proceedings of the IEEE Conference on Computer Vision and Pattern Recognition (CVPR)*, pages 3213–3223.

Diamond, R. and McQuade, T. (2017). Who wants affordable housing in their backyard? an equilibrium analysis of low-income property development. Working paper, Stanford Graduate School of Business.

Dumont, A. M. (2019). Housing affordability in the u.s.: Trends by geography, tenure, and household income. *FEDS Notes*.

Glaeser, E. L. and Gyourko, J. (2003). The impact of building restrictions on housing affordability. *Economic Policy Review*, 9(2):21–39.

Glaeser, E. L., Kim, H., and Luca, M. (2018). Measuring gentrification: Using yelp data to quantify neighborhood change. Technical Report 24952, National Bureau of Economic Research.

Huang, T., Dai, T., Wang, Z., Yoon, H., Sheng, H., Ng, A. Y., Rajagopal, R., and Hwang, J. (2022). Detecting neighborhood gentrification at scale via street-level visual data. In *Proceedings of the 36th AAAI Conference on Artificial Intelligence*.

Karandikar, A. (2024). Shaky foundations – nimbyism's grip on london's housing development. SSRN Working Paper.

Li, X. (2022). Do new housing units in your backyard raise your rents? *Journal of Economic Geography*, 22(6):1309–1352.

Naik, N., Philipoom, J., Raskar, R., and Hidalgo, C. A. (2014). Streetscore: Predicting the perceived safety of one million streetscapes. In *Proceedings of the IEEE Conference on Computer Vision and Pattern Recognition Workshops*, pages 793–799.

NVIDIA (2021). Segformer-b5 model fine-tuned on cityscapes. https://huggingface.co/nvidia/segformer-b5-finetuned-cityscapes-1024-1024. Accessed: 2025-04-28.

Robolyst (2022). Streetview: Download google street view images via api. https://github.com/robolyst/streetview. Accessed: 2025-05-15.

Tiebout, C. M. (1956). A pure theory of local expenditures. *The Journal of Political Economy*, 64(5):416–424.

Vaswani, A., Shazeer, N., Parmar, N., Uszkoreit, J., Jones, L., Gomez, A. N., Kaiser, , and Polosukhin, I. (2017). Attention is all you need. In *Advances in Neural Information Processing Systems*, volume 30, pages 5998–6008.

Wang, W., Wei, F., Dong, L., Bao, H., Yang, N., and Zhou, M. (2020). Minilm: Deep self-attention distillation for task-agnostic compression of pre-trained transformers.

Xie, E., Wang, W., Yu, Z., Anandkumar, A., Alvarez, J. M., and Luo, P. (2021). Segformer: Simple and efficient design for semantic segmentation with transformers. *arXiv preprint arXiv:2105.15203*.

Xu, R. (2023). Difference-in-differences with interference: A finite population perspective. Working paper, Yale University.

6 Appendix

6.1 Neighborhood Character in Housing Minutes

Sentences are converted to sentence embeddings using a all-MiniLM-L6-v2 transformer (Wang et al., 2020). This model generates a 384-dimensional vector representation for each sentence, capturing various latent semantic features. These embeddings are then grouped into $k = 4$ clusters using the K-Means clustering algorithm. Some notable categories are shown in following table.

Cluster #	**% Topic Sent.**	**Manual Label**	**Example**
0	36%	Redevelopment and displacement concerns	"Over the
1	23%	Preserving existing neighborhood amidst new developments	"To our co
2	33%	Historical preservation	"I want to

Table 8: K-Means cluster topics with manual labels and representative sentences.

To visualize the resulting sentence clusters, we reduce the embedding space to the three most variable principal components using PCA, and color points according to their assigned cluster. Cluster 1 predominantly captures language related to "preserving existing neighborhood character amidst new development."

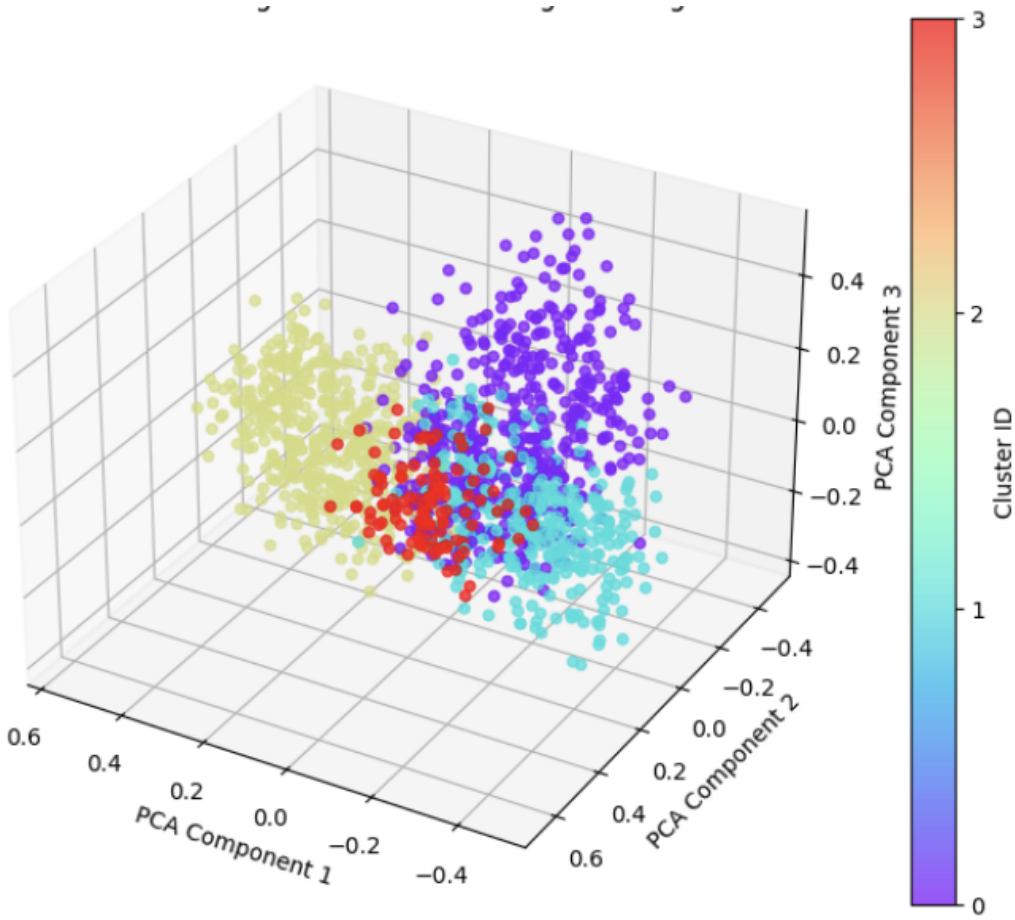

Figure 2: 3D PCA of Sentence Embeddings seperated by K-means Classifier

[give example sentences against because greenspace loss]

6.2 Google Streetview

To acquire the locations of Google Street View panoramas surrounding each multifamily housing project, I construct a 1,200-meter by 1,200-meter grid centered on the project site. This grid is subdivided into a 12×12 array of cells, resulting in subgrids measuring 100×100 meters each. Within each cell, I use Streetview (Robolyst, 2022) to query up n nearby panoramas ($0 \leq n \leq 100$). This process yields multiple panoramas where some panoramas may correspond to the same physical location but captured at different timepoints.

To identify panoramas taken from the same location and camera angle (but at different times), I cluster all panoramas located within 1 meter of one another. I retain only those clusters with at least five unique timestamps, ensuring sufficient historical depth. This is a notable limitation of the data, it gives me less control over the exact points I want to sample,

and I can only rely on the availability of images in a given area, conditional on there being sufficient historical panoramas. After applying this filter, the final sample consists of 145,246 panoramas.

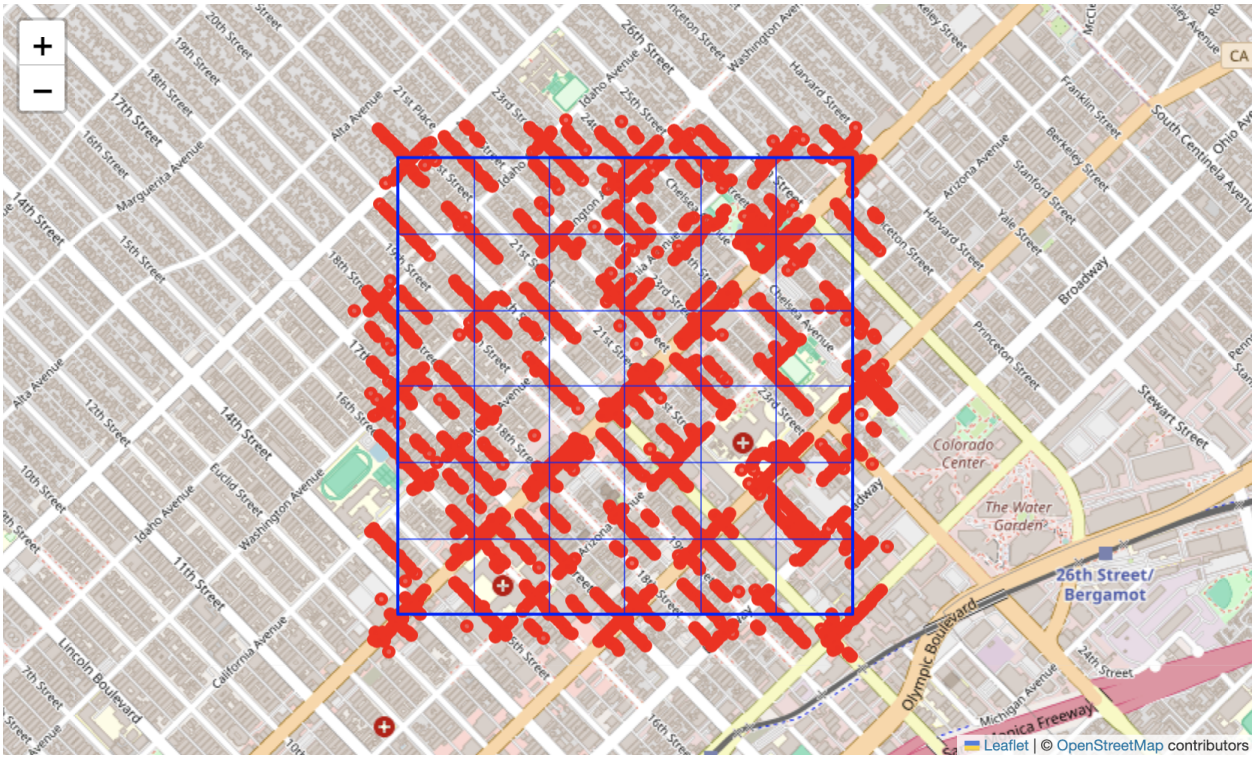

Figure 3: Example of Subgrid Search for a Multifamily Project Located at (34.0319518,-118.4828093)

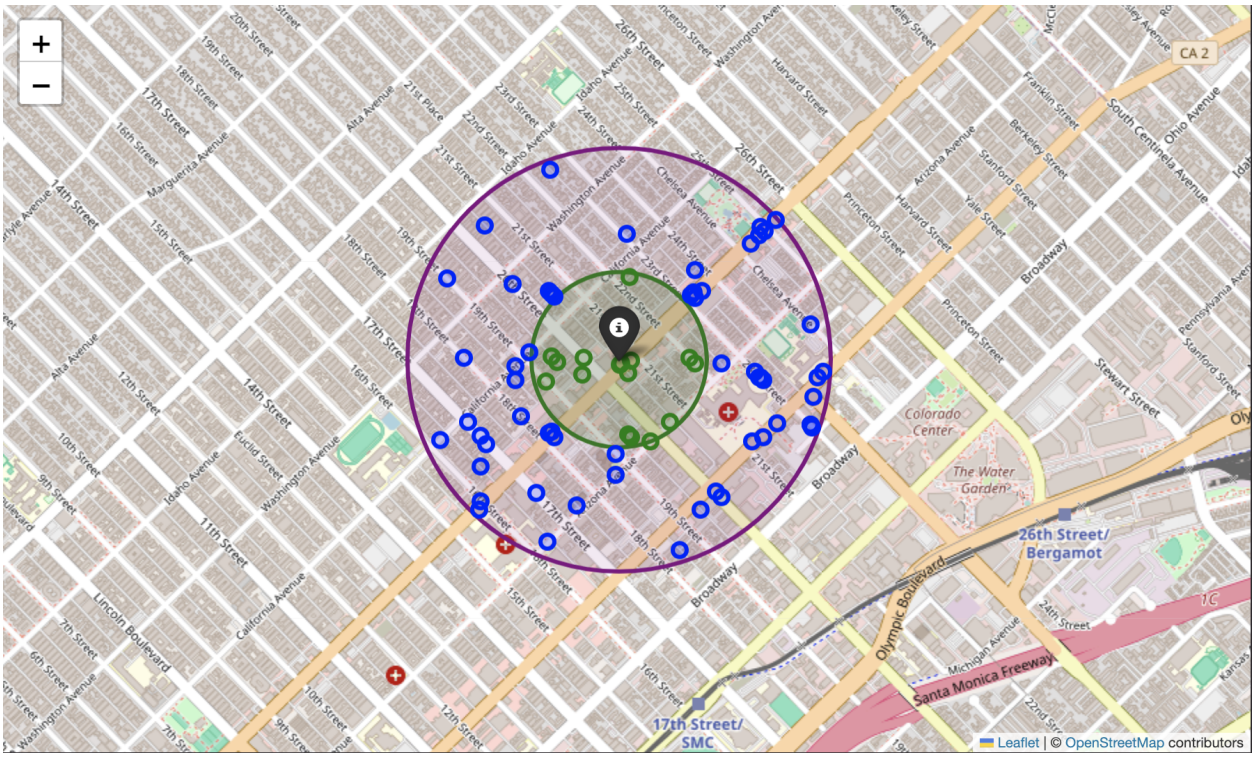

Figure 4: Example of Control and Treatment Spatial Separation for a Multifamily Project Located at (34.0319518,-118.4828093)

6.3 ATT

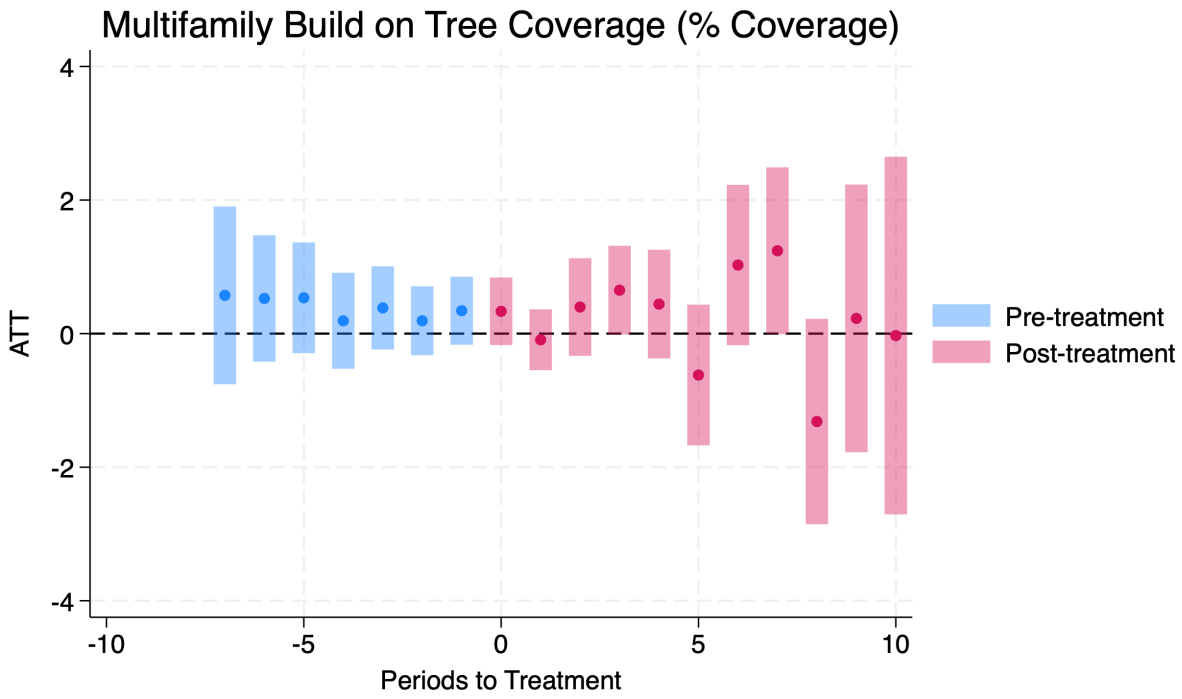

Figure 5: A

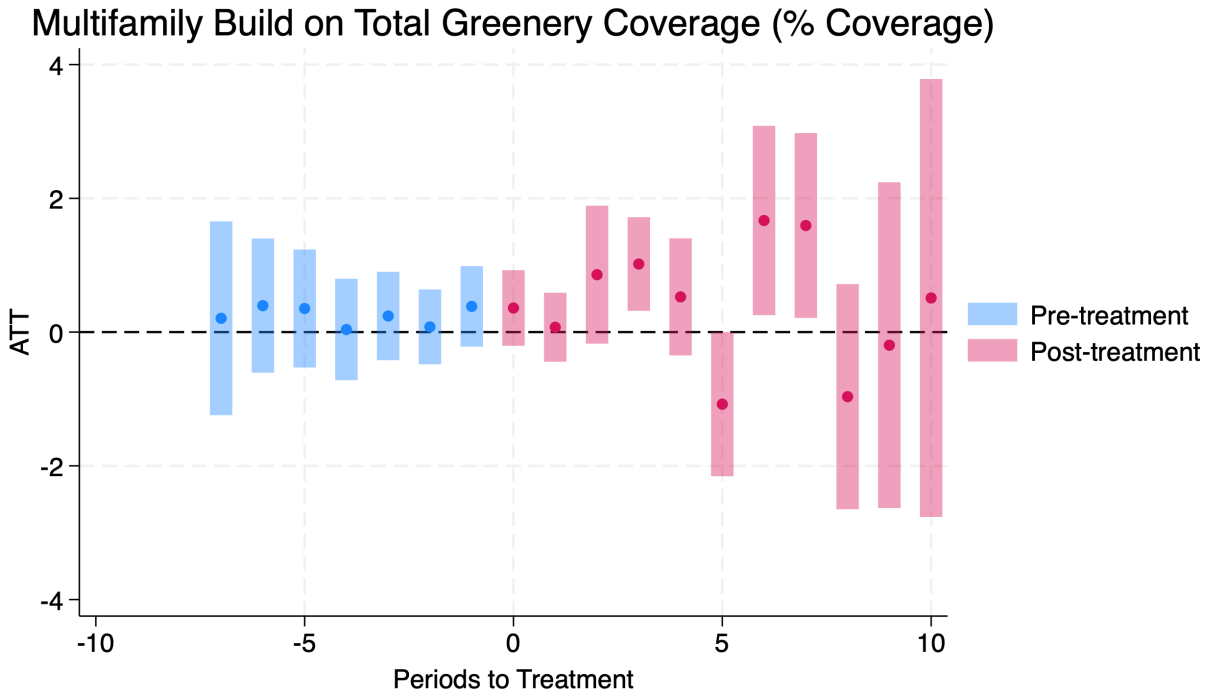
Multifamily Build on Total Greenery Coverage (% Coverage)
ATT
4
2
0
-2
-4
-10
-5
0
5
10
Periods to Treatment
Pre-treatment
Post-treatment

Figure 6: B

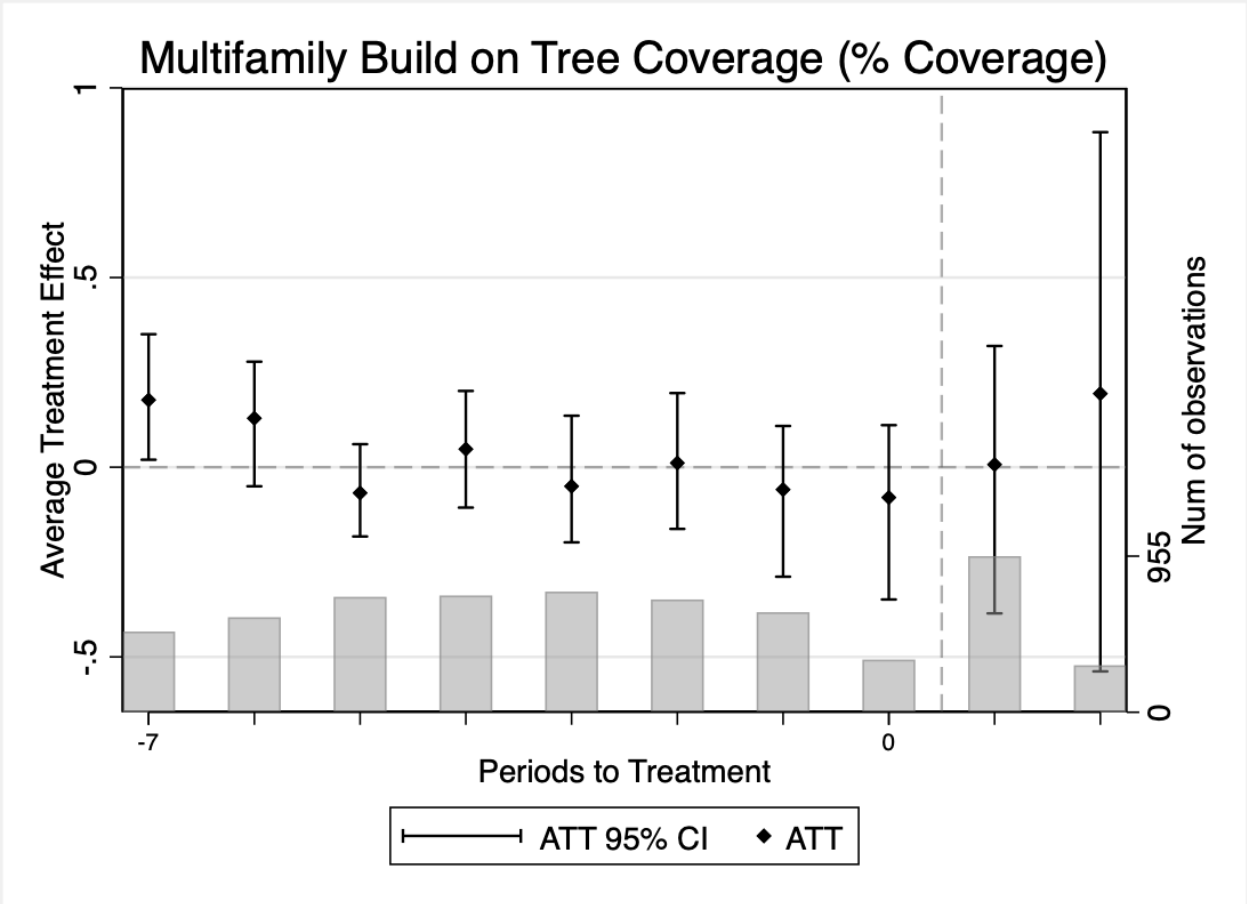
Multifamily Build on Tree Coverage (% Coverage)
Average Treatment Effect
1
.5
0
-.5
Num of observations
955
0
-7
0
Periods to Treatment
ATT 95% CI
ATT

Figure 7: C